Optical Engineering 48(7), 075002 (July 2009)

Stable L-band superfluorescent fiber source using one pump

Wencai Huang
Xiamen University
Department of Electronic Engineering
No. 422 South Siming Road
Xiamen, Fujian 361005
China
E-mail: huangwc@xmu.edu.cn

Xiulin Wang
Jimei University
Department of Physics
No. 185 Yinjiang Road
Xiamen, Fujian 361021
China

Huiying Xu
Zhiping Cai
Xiamen University
Department of Electronic Engineering
No. 422 South Siming Road
Xiamen, Fujian 361005
China

Abstract. We first demonstrate that by inserting an appropriate section of unpumped erbium-doped fiber (EDF) in an erbium-doped superfluorescent fiber source (SFS) of double-pass backward configuration, a stable L-band SFS can be achieved. The fiber-length arrangement of unpumped fiber are shown to have significant effects on the output properties of the L-band SFS. The spectral linewidth is broadened, and the variation of mean wavelength versus pump power is eliminated to achieve a wideband and mean wavelength stable L-band SFS by optimizing the fiber-length ratio of the pumped fiber length to the total fiber length. For a 19-m-long total EDF with fiber-length ratio of 0.84, a mean wavelength stable L-band SFS with a spectral linewidth of 49.6 nm, an output power of 46.3 mW, and a mean wavelength of 1583.20 nm was experimentally achieved. [DOI: 10.1117/1.3168643]

Subject terms: fiber optics amplifiers and oscillators; superfluorescent fiber source; erbium-doped fiber; fiber-optic gyroscope.

Paper 080975R received Dec. 15, 2008; revised manuscript received Apr. 17, 2009; accepted for publication May 26, 2009; published online Jul. 9, 2009. This paper is a revision of a paper presented at the SPIE conference on Optical Instruments and Technology: Advanced Sensor Technologies, November 2008, Beijing, China. The paper presented there appears (unrefereed) in SPIE Proceedings Vol. 7157.

1 Introduction

In the recent decades, superfluorescent fiber sources (SFSs) based on erbium-doped fiber (EDF) amplified spontaneous emission (ASE) had been extensively studied owning to their wide applications for dense wavelength division multiplexing (WDM) device characterization, spectrum-sliced sources, optical sensor systems, fiber-optic gyroscopes (FOG), and optical coherence tomography.[1–3] Especially, many researchers were focused on improving the mean wavelength stability and broadening the linewidth of the SFS for navigation-grad FOG applications. In the first few years, conventional wavelength band (C-band, 1525–1565 nm) EDF SFSs have been studied intensively and the double-pass backward (DPB) configuration has been demonstrated to offer the highest output power, better mean wavelength stability, and broader linewidth.[4] In the recent years, most researchers have been focusing on the long wavelength band (L-band, 1565–1605 nm) SFS in order to increase its output power, spectral linewidth, and wavelength stability to cater to the demand of band expansion of the fiber-optic communication window.[5–8] The mean wavelength stability of L-band SFS was not included in the research, although it is more suitable in FOG application for its potential larger linewidth to achieve a higher value of signal-to-noise ratio. Recently, we have proposed a stable L-band SFS using a double-pass bidirectional pumped configuration and synchronous pumping technique.[9,10] However, the configuration presented in Refs. 9 and 10 is quite complicated. Another disadvantage of the synchronous pumping technique is that the mean wavelength stability becomes sensitive to the small variations in the power-splitting ratio of the power splitter. The wavelength stable L-band SFS with a simpler configuration and new technique is necessary to accelerate its application in all-fiber FOG.

In this paper, we first demonstrate a new technique by adding an unpumped EDF in a single-backward pumped SFS configuration for an L-band SFS of broadening linewidth and stable mean wavelength. The configuration is based on the conventional DPB configuration, while using an additional unpumped fiber between the WDM coupler and the isolator at the end of the output terminal. It is proved that the proposed design can not only have the characteristic of mean wavelength insensitive to pump power operation but also has a broadening linewidth with the optimized structural parameters. To the best of our knowledge, such a technique is simpler than those reported before for a stable L-band SFS and shown effective to have a broad linewidth with moderate output power.

2 Configuration of Single-Backward Pumped L-Band SFS

Figure 1 illustrates the suggested single backward pumped L-band SFS. The source consists of two sections of EDF (EDF1 and EDF2), a 980-nm pump laser diode (LD), a 980/1590 nm WDM, a fiber mirror made by a 3-dB broadband couple, and an optical isolator at the output port. The section of EDF1 is backward pumped by the 980-nm LD, and the other one (EDF2) is unpumped and separated from EDF1 by the WDM. We define the total length of EDF as

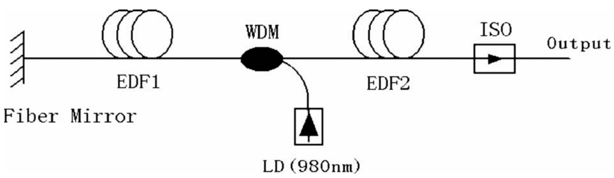

Fig. 1 Proposed L-band SFS using single backward pumped technique.

$L = L_1 + L_2$, where L_1 and L_2 are referred to as the first stage (EDF1) and the second stage (EDF2) lengths, respectively. The fiber-length ratio of EDF1 to the total length is defined as $R_L = L_1 / L$. The EDF used in the numerical simulations and experiments is the heavily doped LRL fiber (Lucent Technologies, type number L12403) with a peak absorption of 27–33 dB/m at 1530 nm, mode field radius of 5.2 μm, cutoff wavelength of 1100–1400 nm, and numerical aperture of 0.25.

The principle of the proposed L-band SFS with backward pumped configuration can be explained as follows. Generally, the L-band ASE is realized using a long fiber with a forward-pumped configuration.[5] Namely, the C-band ASE generated by the anterior fiber inject into the later fiber section is to be a second pump source, then an L-band ASE will be attained in the output. For the configuration presented in this paper, the backward C-band ASE of EDF1 is transfused into the output stage EDF2 to be a second pump source, so an L-band SFS output can be obtained in the end of EDF2 with an appropriate fiber-length arrangement.

3 Simulation and Experimental Results

Previous simulations and experiments have indicated that the simulation results obtained by the commercial amplifier simulation package OASIX are quite accurate.[9,11–13] Therefore, the OASIX is used to perform the simulations of the proposed configuration as shown in Fig. 1 in order to gain insight into and to optimize its output properties. It is noted that the mean wavelength of the ASEs is computed by

$$\bar{\lambda} = \frac{\sum_{i=1}^{n} p(\lambda_i)\lambda_i}{\sum_{i=1}^{n} p(\lambda_i)} \tag{1}$$

and the spectral linewidth is defined as

$$\lambda = \frac{\left[\sum_{i=1}^{n} \Delta\lambda_i P(\lambda_i)\right]^2}{\sum_{i=1}^{n} \Delta\lambda_i P(\lambda_i)^2}, \tag{2}$$

where λ_i is the wavelength of the i'th ASE wave, $P(\lambda_i)$ is the power in the i'th ASE wave of the emission spectrum, n is the number of discrete ASE wavelengths, and $\Delta\lambda_i$ is the spectral width represented by the i'th ASE wave.

There is no doubt that the output ASE spectrum is largely dependent on the total fiber length used. Therefore, the total fiber length is initially optimized to obtain a flat L-band spectrum output. The effective reflectivity of the fiber mirror is selected to be 90%, and the total pump power is set to 100 mW. For different fiber-length ratios, R_L, the output spectra of the L-band SFS at various EDF lengths are simulated. The result indicates that for different R_L, the optimal EDF length for the flat L-band spectrum (i.e., for the maximal value of linewidth) is ~19 m. Hence, the total EDF length is fixed at 19 m of the L-band SFS in the following simulations.

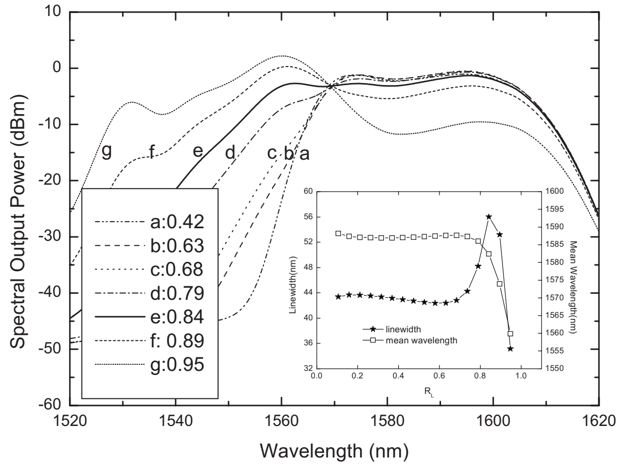

Fig. 2 Simulated output spectra in different R_L cases. Inset: Linewidth and mean wavelength versus R_L.

The effects of the fiber-length ratio R_L on the output spectrum have been addressed. Figure 2 shows the output spectra for the configuration of different R_L with a pump power of 100 mW. Curves a–g correspond to $R_L = 0.42$, 0.63, 0.68, 0.79, 0.84, 0.89, and 0.95, respectively. The variation of the output linewidth and the mean wavelength versus R_L are shown in the inset of Fig. 2. As apparent from Fig. 2, when the $R_L < 0.7$, R_L has little influence on the L-band spectral shape. However, when R_L changes from 0.7 to 0.85, the spectral intensity increases significantly in the short-wavelength range, and decreases in the long-wavelength range, gradually. The mean wavelength shifts toward shorter wavelengths, and the linewidth increases to the maximum value when R_L is adjusted to ~0.84. If $R_L > 0.85$, then the SFS is no longer an L-band fiber source; the output spectrum shifts to C-band mostly with a decreasing of the mean wavelength and the linewidth.

The reason for the changes of the spectral characteristics resulting from the different values of R_L can be illustrated as follows. In the L-band SFS, shown in Fig. 1, EDF1 is backward pumped. The output from EDF1 produced by the direct pump of the LD, which is called ASE1+, is C-band ASE. ASE1+ is injected into EDF2 through the WDM to pump EDF2. In EDF2, there are two different ASEs in opposite directions generated by ASE1+, referred to as ASE2+ and ASE2−, respectively. ASE2− passes through EDF2 and EDF1 and then goes back again when it reaches the fiber mirror. Thus ASE2− turns to be ASE3+ when it goes into EDF2, as shown in Fig. 3. The total output of the SFS is composed of two components: ASE2+, which is generated directly by ASE1+, and ASE3+, which is generated by the ASE2− passing through the fiber. The wave-

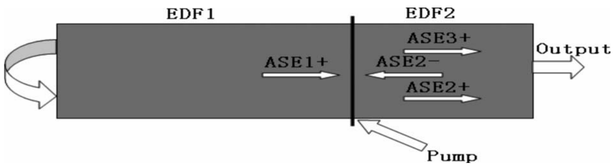

Fig. 3 Schematic diagram of Fig. 1

length ranges and the proportion of the two components determine the output characteristic of the spectrum. When $R_L<0.7$, the length of EDF2 is long enough to make ASE2+ and ASE3+ shift to the L band. Thus, the mean wavelength and the spectrum output are stabile in the L band and the linewidth and mean wavelength remain nearly unchanged. When R_L is in the region of 0.7–0.85, the wavelength range of ASE3+ is also in the L band while the fiber length of EDF2 now is not long enough to shift all the ASE2+ into the L band. The intensity and the mean wavelength of ASE2+ and ASE3+ act together to make the output spectrum broaden to the C band, and this results in the linewidth increasing rapidly and the mean wavelength shifting toward shorter wavelengths. When $R_L>0.85$, the length of EDF2 keeps decreasing. In this process, the wavelength ranges of ASE2+ keep moving to shorter wavelengths (C-band) and the intensity of ASE2+ keeps augmenting, which lead to the fast decrease of the mean wavelength and the linewidth of the total output spectrum. By the competition between ASE2+ and ASE3+, the maximum linewidth is attained with R_L of 0.84, corresponding to $L_1=16$, $L_2=3$ m.

The variation of the mean wavelength versus pump power is investigated. Figure 4 compares the mean wavelength profiles against pump power and shows the high tunability of the mean wavelength against pump power characteristic by adjusting the fiber length ratio R_L. The total fiber length is fixed at 19 m. It is shown clearly in Fig. 4 that when R_L is lower, for the cases of $R_L=0.42$ ($L_1=8$, $L_2=11$ m), and 0.63 ($L_1=12$, $L_2=7$ m), the mean wavelength keeps decreasing with the increase of pump power. However, with R_L of 0.68 ($L_1=13$, $L_2=6$ m), 0.79 ($L_1=15$, $L_2=4$ m), and 0.84 ($L_1=16$, $L_2=3$ m), the mean wavelength increases to a maximum and then decreases as pump power increases. When R_L is further increased to a value as high as 0.89 ($L_1=17$, $L_2=2$ m), the pump power–independent mean wavelength operation disappeared. The mean wavelength keeps increasing with the pump power within the given largest pump power of 225 mW. The results of Fig. 4 demonstrate the high tunability of the mean wavelength against pump power characteristic by adjusting the fiber length ratio R_L. The pump power independent mean wavelength operation with $\partial\bar{\lambda}/\partial P=0$ is able to exist for the suggested SFS source by selecting a suitable R_L within a certain range. Furthermore, it should be noted that the total pump power to obtain a stable mean wavelength is different in the different pump ratios. Figure 5(a) illustrates the required pump power for obtaining stable mean wavelengths in different R_L, while Fig. 5(b) gives the corresponding available linewidth and pumping efficiency. We can see clearly from Fig. 5(a) that pump power-independent mean wavelength operation cannot be always achieved by the proposed single pumping scheme. Too low or too high fiber-length ratios are not satisfactory for obtaining a stable SFS. The mean wavelength decreases monotonously with pump power when $R_L<0.6$, while the mean wavelength increases monotonously with pump power when $R_L>0.9$. The results show that a fiber-length ratio between 0.6 and

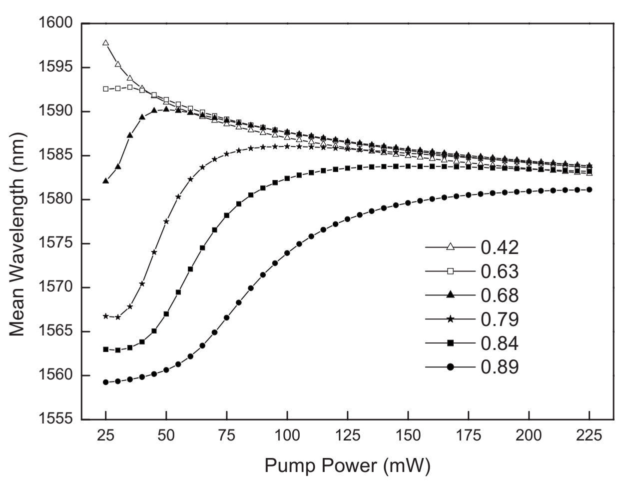

Fig. 4 Calculated mean wavelengths versus pump power.

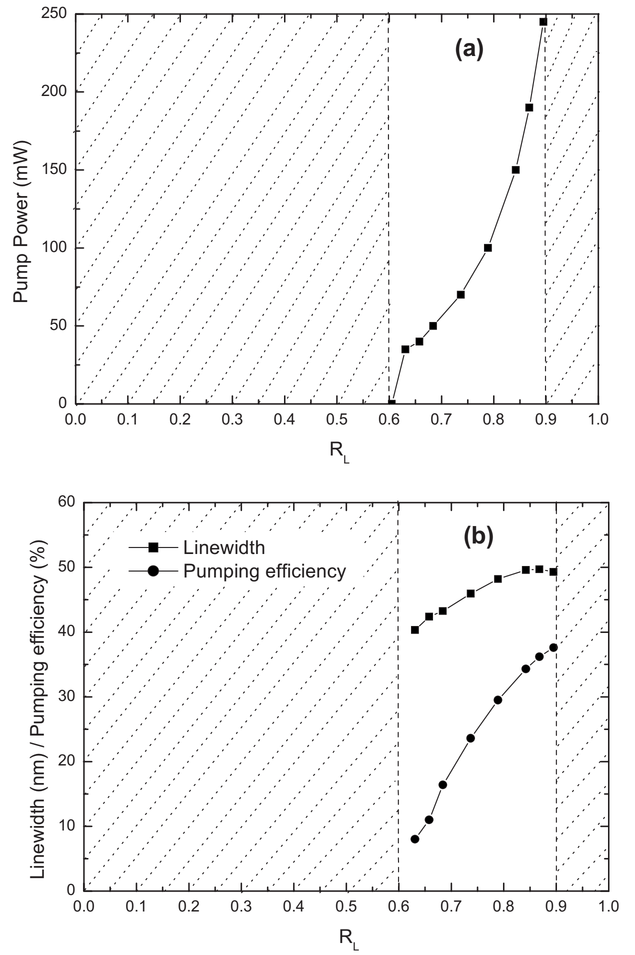

Fig. 5 (a) The pump power for stable mean wavelengths and (b) corresponding spectral linewidth and pumping efficiency against R_L.

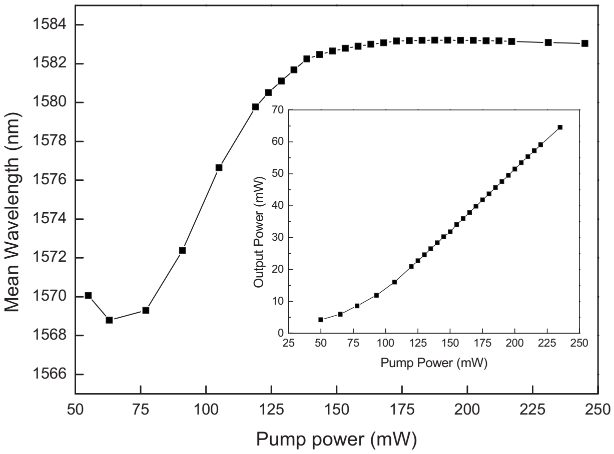

Fig. 6 Measured mean wavelength and output power versus pump power.

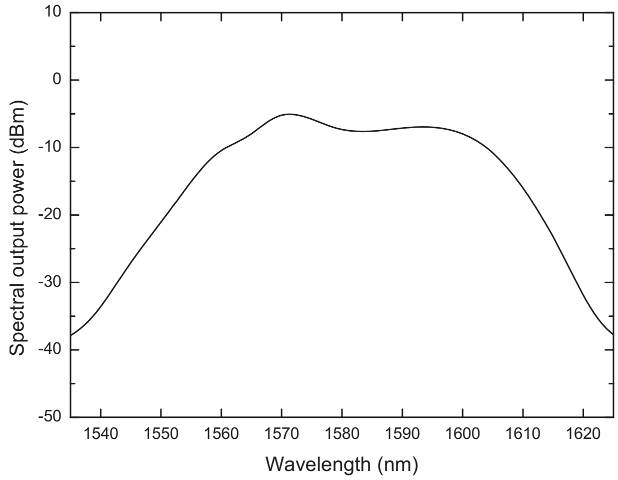

Fig. 7 Measured output spectrum for 187.5-mW pump power.

0.9 is suitable to achieve a stable L-band SFS using this design. Figure 5(a) also indicates that the larger the value of R_L is, the higher the pump power needed to get the stable mean wavelength operation. Figure 5(b) guides us to select the optimization of R_L to obtain the best output characteristics of the linewidth and pumping efficiency. The result of Fig. 5(b) shows that pumping efficiency increases as R_L increases. However, the linewidth is saturated when the R_L is ~0.85. Hence, the optimum fiber-length ratio, R_L, was selected to be 0.84 (i.e., $L_1=16$ and $L_2=3$ m) to achieve a mean wavelength stability L-band SFS with a high pumping efficiency, a maximum linewidth, and a moderate pump power.

Figure 6 shows the measured mean wavelength as a function of pump power of the suggested L-band SFS. The output spectrum was measured using an Advantest optical spectrum analyzer (OSA) that divided the spectrum into 1000 discrete points. The mean wavelength and linewidth of the spectrum are computed by Eqs. (1) and (2). Stable mean wavelength operation was observed when the pump power was 187.5 mW, corresponding to a mean wavelength of 1583.20 nm. The experimental results show good agreement with the simulations, with quantitative discrepancies attributable primarily to splice loss, insertion loss in the WDM coupler, etc. Figure 6 also shows the output spectrum power against pump power. An output power of 46.3 mW, corresponding to a pumping efficiency of 24.7% was achieved for the stable mean wavelength operation under pump power of 187.5 mW. Figure 7 shows the obtained output L-band spectrum of 187.5-mW pump power. It can be seen clearly that the linewidth is obviously broadened to the edge of C-band, corresponding to a spectral linewidth of 49.6 nm. As compared to the mean wavelength stability L-band SFS demonstrated in Ref. 10, the proposal of a single pumping scheme to achieve a mean wavelength stable L-band SFS is much simpler and with a larger tolerance in the structure parameters. The advantages of high tunability of the mean wavelength and large linewidth of the proposed single-pumped L-band SFS make it more useful in a high-precision FOG application.

4 Conclusion

In conclusion, we have demonstrated that a new single-pumped erbium-doped L-band SFS can not only have the characteristic of mean wavelength insensitive to pump power operation but also a large linewidth by inserting an appropriate section of unpumped EDF in front of an isolator at the end of the output terminal. For a 19-m-long total EDF with fiber-length ratio of 0.84, a mean wavelength stable L-band SFS having spectral linewidth of 49.6 nm, an output power of 46.3 mW, and a mean wavelength of 1583.20 nm was experimentally demonstrated. There was good agreement between experiment and theory. To the best of our knowledge, such a technique is simpler than those reported previously for a stable L-band SFS and has a broad linewidth with moderate output power. Such a single-pumped stable L-band SFS should be useful in WDM systems, FOGs, and fiber-optic sensor systems.

Acknowledgments

This work was supported by the Program for New Century Excellent Talents in Fujian Province University under Grant No. X07204, the Scientific and Technical Project of Fujian Provincial Department of Education under Grant No. JA08138, and the Key Scientific and Technical Innovation Project of Xiamen University under Grant No. K70007. The authors thank Benrui Zheng for some useful discussion.

References

1. P. F. Wysocki, M. J. F. Digonnet, B. Y. Kim, and H. J. Shaw, "Characteristics of erbium-doped superfluorescent fiber sources for interferometric sensor applications," *J. Lightwave Technol.* **12**, 550–567 (1994).
2. C. D. Su and L. A. Wang, "Multiwavelength fiber sources based on double-pass superfluorescent fiber sources," *J. Lightwave Technol.* **18**, 708–714 (2000).
3. P. F. Wysocki, M. J. F. Digonnet, and B. Y. Kim, "Spectral characteristics of high-power 1.5 μm broad-band superluminescent fiber sources," *IEEE Photonics Technol. Lett.* **2**, 178–180 (1990).
4. L. A. Wang and C. D. Chen, "Stable and broadband Er-doped superfluorescent fiber sources using double pass backward configuration," *Electron. Lett.* **32**, 1815–1817 (1996).
5. J. H. Lee, U. C. Ryu, and N. Park, "Passive erbium-doped fiber seed photon generator for high-power Er3+-doped fiber fluorescent sources with an 80-nm bandwidth," *Opt. Lett.* **24**, 279–281 (1999).

6. S. C. Tsai, C. M. Lee, S. Hsu, and Y. K. Chen, "Characteristic comparison of single-pumped L-band erbium-doped fiber amplified spontaneous emission sources," *Opt. Quantum Electron.* **34**, 1111–1117 (2002).
7. S. C. Tsai, T. C. Tsai, P. C. Law, and Y. K. Chen, "High pumping efficiency L-band erbium doped fiber ASE source using double pass bidirectional pumping configuration," *IEEE Photonics Technol. Lett.* **15**, 197–199 (2003).
8. S. P. Chen, Y. G. Li, J. P. Zhu, H. Wang, Y. Zhang, T. W. Xu, R. Guo, and K. C. Lu, "Watt-level L band superfluorescent fiber source," *Opt. Express* **13**, 1531–1536 (2005).
9. X. L. Wang and W. C. Huang, "Wavelength stability optimization of L-band superfluorescent fiber source," *Opt. Eng.* **44**, 060504 (2005).
10. W. C. Huang, X. L. Wang, B. R. Zheng, H. Y. Xu, C. C. Ye, and Z. P. Cai, "Stable and wideband L-band erbium superfluorescent fiber source using improved bidirectional pumping configuration," *Opt. Express* **15**, 9778–9783 (2007).
11. OASIX v3.0: Lucent Technologies erbium doped fiber devices simulation software.
12. M. D. Dominique, G. Lew, P. M. Robert, and K. B. William, "Wavelength stability characteristics of a high-power, amplified superfluorescent source," *J. Lightwave Technol.* **17**, 1415–1422 (1999).
13. P. Z. Zatta and D. C. Hall, "Ultra-stability two-stage superfluorescent fiber source for fiber optics gyroscope," *Electron. Lett.* **38**, 406–408 (2002).

Wencai Huang received his PhD in optics from University of Science and Technology of China in 2003. He is currently an associate professor in the Department of Electronics Engineering at Xiamen University. His research interests are in the areas of fiber optics communication devices, fiber lasers and amplifiers, fiber broadband light sources, and femtosecond soliton generation in PCF and pulse compression. He has published more than 40 papers in optical journals and conferences.

Biographies and photographs of the other authors not available.